EFFECT OF SILVER ION REDUCTION ON ELECTRICAL MODULUS OF CHITOSAN-SILVER TRIFLATE SOLID POLYMER ELECTROLYTE MEMBRANE

Soran Kamal[a] and Sleman Qadir[a]

Keywords: silver; electrical modulus; polymer electrolyte; chitosan; silver triflate

Utilizing impedance spectroscopy, chitosan-based solid polymer electrolyte containing CF_3SO_3Ag was investigated for their electric modulus properties. Using the highest conductivity sample, the lowest conductivity relaxation time (τ_σ) was determined. The high capacitivity of the material is shown by the electrical modulus of the real part. A non-Debye type relaxation is predicted by the asymmetric peak of electric modulus's imaginary part (M''). Utilizing Argand plot, a deformed arc for the relaxation times distribution is demonstrated. Silver nanoparticles formed from silver ions causes a rise in the values of M' and M'' above 358 K. The ultraviolet-visible (UV-vis) absorption and complex impedance of silver nanoparticles in chitosan-silver triflate solid electrolyte are temperature dependent. Transmission electron microscopy (TEM) confirmed the silver nanoparticles formation. The dynamical relaxation process for a particular composition is proven by the scaling behavior of M'' spectra to be independent of temperature. The conductivity relaxation is shown by a β exponent to be non-exponential.

* Corresponding Authors
E-Mail: soran3979@gmail.com
[a] KSCIEN Organization for Scientific Research, Hamdi Street, Sulaimani, Iraq.

Introduction

Very intriguing classes of solid-state coordination compounds are polymer electrolytes that utilize solid but flexible membranes for ionic conductivity.[1] Because of the attractive interaction between cations and chains, chain polymers can act as solvents for certain salts if they have electronegative atom (nitrogen or oxygen) in their repeating units.[2] Chitosan polymers contain both N and O atoms in their chains[3] are used as solid electrolytes in electrochromic displays, sensors, fuel cells and batteries.[4,5] Despite the intensive studies, the mechanism for their conductivity is still not clarified completely.[6] The amorphous phase is the main conductive phase, despite the coexistence of crystalline and amorphous phases.[7] Little is understood about the coupling between ion transport and polymer segmental relaxation in polymer electrolytes and could be the key for new discoveries.[8]

In the polymer electrolytes, both dipoles and charge species affect the relaxation dynamic and frequency dependent conductivity.[9] Electric modulus formalism M'' can be used as an environment for studying relaxation dynamics, specifically dielectric relaxation.[10] M'' displays a pronounced peak, leading to modulus representation and associating the extent of conductivity with time scale τ.

Despite the well establishment of relations between the various quantities, yet there is still debate on modulus representation.[11] When the electric displacement is constant, from the physical viewpoint, the relaxation of electric fields in the material is correspondent to the electrical modulus.[12] Emphasizing small features at high frequencies and suppressing the high signal intensity associated with electrode polarization is the main benefit of modulus representation.[11] Therefore, studying relaxation times and conductivity in polymers and ionic conductors can be achieved through electric modulus spectra.[13]

In the chitosan-silver triflate polymer electrolyte thin film preparations, commercial chitosan was used as a base polymer containing amine and hydroxyl functional groups and suitable for solid polymer electrolyte preparation.[14] Silver salts like $AgSbF_6$, CF_3SO_3Ag, $AgBF_4$ and $AgClO_4$ were tested in polymer hosts like and poly(vinylpyrrolidone) (PVP), poly(ethylene oxide) (PEO) and poly(2-ethyl-2-oxazoline)(POZ) to make silver-based polymer electrolytes.[15,16] Olefin transport is facilitated essentially by nitrogen and oxygen atoms contained within polar polymer chains, and silver metal particles were formed due to the reduction of silver ions.[17,18]

Due to these properties, the effect of silver nanoparticle reduction from silver ions on the properties of electrical modulus of chitosan-silver triflate solid electrolyte is studied in this paper over a wide range of temperature and frequency.

Experimental

Solid polymer electrolyte (SPE) thin film preparation

Silver triflate (CF_3SO_3Ag) (Fluka, ε99 purity, Germany, CAS No. 2923-28-6) and chitosan from crab shells (ε75 % deacetylated, Sigma Aldrich, USA, CAS No. 9012-76-4) were used as raw materials. Solution cast technique with the solvent being acetic acid (1 %) is used for the preparation of solid polymer electrolyte (SPE) films. Chitosan (1 g) is dissolved in acetic acid solution and fixed in the current system. Varying amount of silver triflate (CF_3SO_3Ag) ranging from 2 to 10 wt. % in steps of 2 wt. % is added to this system to adjust different compositions of chitosan-

silver triflate electrolyte in weight percent ratios; 98:2, 96:4, 94:6, 92:8 and 90:10 for chitosan: CF_3SO_3Ag and 100:0 for pure chitosan acetate. To obtain a homogenous solution, the mixture is continuously stirred until said result is obtained. In room temperature, the solutions are left to dry in different Petri dishes after casting, in order to form the films, then further drying is done by transferring into desiccators. The result is a solvent-free and mechanically stable film.

Complex impedance measurement

Characterization of the materials electrical properties is done through the complex impedance spectroscopy. Small discs of 2 cm diameter are made from the SPE films, and to ensure proper electrical contact between the sample and electrodes, two clean stainless steel and circular shaped electrodes are used under spring pressure. This solves the problem of air interstices between the electrodes and the sample interface. HIOKI 3531 Z Hi-tester (made in Japan, No.1036555) is used to measure the impedance of films in the frequency range from 50 to 1000 kHz. The imaginary and real parts of the impedance is calculated and measured by the software. Using b equations below, the real (M') and imaginary (M'') parts of complex electric modulus (M^*) is evaluated by the use of the real (Z') and imaginary (Z'') part of complex impedance (Z^*) [19]:

$$M^* = 1/\varepsilon^* = M' + jM'' = j\omega C_0 Z^*$$

$$M' = \frac{\varepsilon'}{\varepsilon'^2 + \varepsilon''^2} \quad \text{and} \quad M'' = \frac{\varepsilon''}{\varepsilon'^2 + \varepsilon''^2}$$

$$Z^* = Z' - jZ''$$

where

C_0 is the vacuum capacitance and given by $\varepsilon_0 A/l$,

A is the area of the film,

l is the thickness and

The angular frequency is represented by ω and is equal to $\omega = 2\pi f$; the applied field's frequency is f.

UV-Vis and TEM characterization

The absorbance mode of Jasco V-570 UV-Vis-NIR spectrophotometer (Japan, Jasco SLM-468) is used to record the UV spectra of chitosan-silver triflate electrolyte films. An LEO LIBRA (Germany, 120 EFTEM, accelerating voltage 120 kV) TEM instrument was used. The excess solution was removed by a filter paper from the dried chitosan-silver triflate electrolyte solution placed on a carbon-coated copper grid at room temperature.

Results and discussions

Concentration dependence of M″ spectra

The M'' spectra frequency dependencies for compositions with different silver triflate content at 303 K are shown in Figure 1. In the highest conducting sample could be observed higher frequencies for maximum M'' peaks. Possibly due to polar group relaxations especially at low frequency, pure chitosan and chitosan-silver triflate (98:2) may show more than one peak. At higher salt concentrations, because of the motion and high free charge carrier concentration within the material, these peaks are disappeared. Consequently, the low-frequency relaxation can be hidden due to a high DC conductivity that is produced.

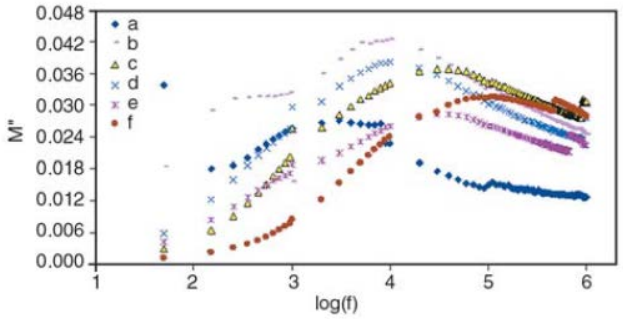

Figure 1. Concentration dependence of M'' for (a) pure chitosan acetate (100:0), (b) 98:2, (c) 96:4, (d) 94:6, (e) 92:8 and (f) 90:10 for chitosan: CF_3SO_3Ag at 303 K.

Broadening of the peaks suggests a non-Debye type relaxation, representing the conductivity relaxation peaks distribution of the free charges.[20] As conductivity increases, the relaxation times decrease and causing shifting to higher frequencies.[21] Through the relation $2\pi f_{max}=1/\tau_\sigma$, we can calculate the conductivity relaxation times, were f_{max} is a frequency corresponding to M''_{max} and τ_σ is the conductivity relaxation time. Figure 2 shows silver triflate concentration function as a variation of τ_σ as the salt concentration increases up to 4 wt. % CF_3SO_3Ag, the conductivity relaxation ties decrease. We can deduct from the results, especially at the 4-8 wt. % concentration that there is a competition between the ion associations and dissociations — a charge carriers concentration increases from 8 wt. % CF_3SO_3Ag to 10 wt. % CF_3SO_3Ag explains the significant drop in conductivity relaxation times, i.e., as the number of mobile charge carriers increases, the conductivity increases.

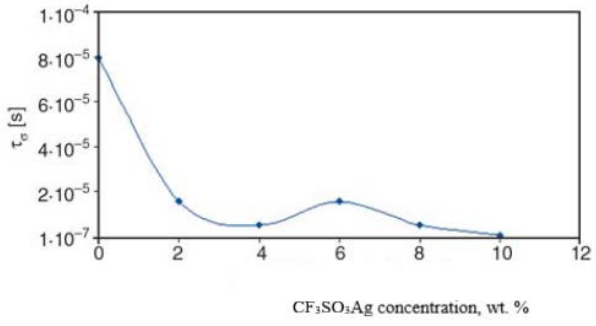

Figure 2. Concentration dependence of conductivity relaxation time (τ_σ) at 303 K

M′ and M″ frequency dependence at selected temperatures

The imaginary and the real part's frequency dependence of the complex modulus for the sample with the highest conductivity (90:10) at various temperatures are shown in Figure 3 and 4. Equations given were used to calculate the imaginary and real parts of the complex modulus.

Using the representation of electrical modulus (M^*), the conductivity behavior in regards to conductivity relaxation time can be interpreted conveniently. Ionic conductivity analysis is commonly done by the representation of M^* through ionic process association with conductivity relaxation time.[22] M' are very small at lower frequencies, as illustrated by Figure 3, the electrode polarization is close to zero thus can be neglected.[23,24]. At higher frequency, M' increases until reaching the maximum value of M_∞ due to the wide range of relaxation process frequencies.[25] The spread of conductivity relaxation over a range of frequencies explains the observed dispersion and pointing to the occurrence of relaxation time and the presence of a loss of peak at the same time in the imaginary part diagram of electric modulus versus frequency. ε′ in complex permittivity (ε*) is equivalent to M' in complex electric modulus (M^*) and this explains the peak absence in M' diagram, i.e., the capability of the material for energy storage is represented by M'. The charge carriers and mobility of the polymer increase with increasing the temperature and due to this, the M' values are decreased.

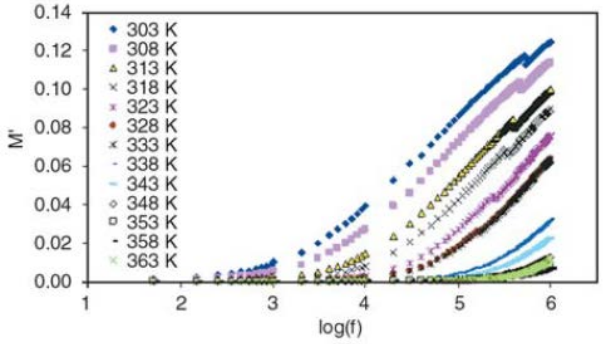

Figure 3. Frequency dependence of *M'* at different temperatures for chitosan-silver triflate=90:10 composite

With increasing the temperature, the orientation of molecular dipoles and charge carriers become easier. It is possible that the electrode polarization effect with its large value of capacitance causes M'' to exhibit low values at low frequencies.[26] A large amount of charge carriers are accumulated on the interface of electrode/solid polymer electrolyte. The peaks can be seen at high frequencies (Figure 4). The non-Debye behavior is illustrated by the asymmetric and board peaks on both sides of maxima. The region on the right of the peak are carriers that are mobile on short distances and are confined to potential walls, while the region to the left of the peak is carriers that are mobile over a long distance.[24]

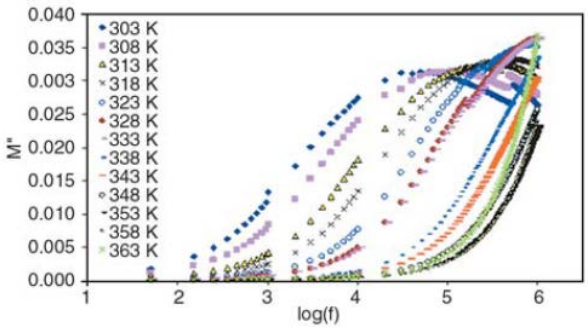

Figure 4. Frequency dependence of M'' at different temperatures for chitosan-silver triflate (90:10) composite

Experimental frequency limitation explains the disappearing of the M'' peaks at higher temperatures. The formation of silver nanoparticles from the reduction of silver ions contributes to the rise of both M' and M'' above 358 K. The function of temperature at a fixed frequency can be used to study M' and M'' as a way for studying silver ion reduction to silver nanoparticles.

The best conductivity relaxation time of ions (τ_σ) is the relaxation frequency associated with the peak. Figure 5 demonstrates the relationship of reciprocal temperature and log(f_{max}). The activation energy (Arrhenius behavior), E_a = 1.16 eV.

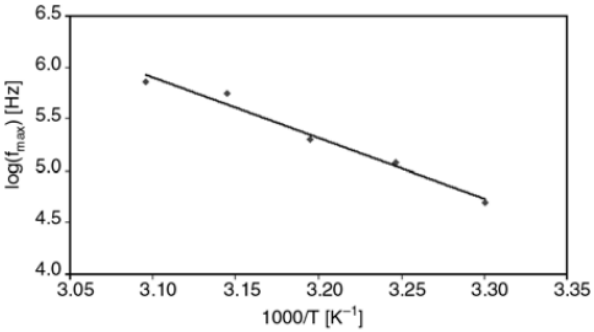

Figure 5. Temperature dependence of relaxation frequency

The rise in the mobility of ionic carriers with rising temperature causes a reduction in relaxation time. The points form almost a straight line, the regression value R^2 is 0.996.

Argand plots analysis

In polymer electrolytes, the nature of the relaxation process can be studied by Argand plot demonstration. The dependence of Argand plot on temperature is shown in Figure 6.

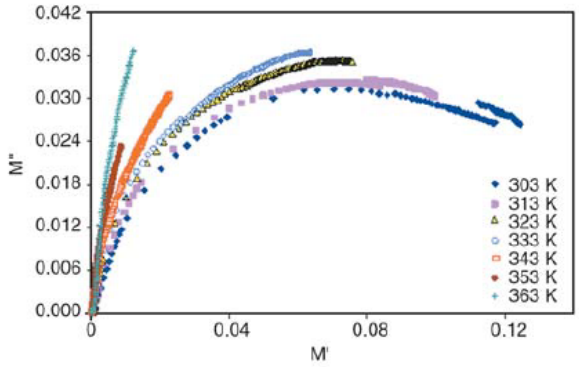

Figure 6. Argand plots for chitosan-silver triflate (90:10) at different temperatures

It can be concluded that the Debye model (single relaxation time) fails to explain the half semicircle curves of Argand plot shown in Figure 6. In this situation, especially in polymers to understand the experimental data, a distribution of relaxation time becomes mandatory.

The possible reasons for this distribution type are space charge polarization, hopping, the ellipsoidal shape of polar groups and the presence of inhomogeneity.[27] At lower temperatures, the Argand plot shows deformed arcs with centers localized below the horizontal axis. The electric relaxation of material corresponds with this position of the centers as well as distribution and intercorrelation of activation energy and relaxation time.[28] There is a shift in Argand curves when the temperature rises (Figure 6). This can be explained with increasing of ionic mobility with the increased conductivity resulting from risen temperature and both Z' and Z'' increase, subsequently. At 363 K, the resistance within the sample increases, since a large amount of silver nanoparticles form from silver ions reductions, causing an increase on M''–M' curves.

The dependence of M′ and M″ on t

he temperature shown in Figure 7a and 7b. Until 358 K due to a rise of ionic conductivity, M' and M'' decrease as the temperature rises because of the dominance of silver ions. However, above 358 K, a large amount of silver ions transform into silver nanoparticles causing M' and M'' to increase with rising the temperature. The ionic motion is hindered by the increase of resistance within the sample caused silver nanoparticles.

The complex impedance plots can detect the presence of silver nanoparticles within the sample. Phase transitions, interfacial effects in polymers and complex systems, molecular mobility and conductivity mechanisms can also be efficiently studied by electrochemical impedance spectroscopy.[29]

Figure 8 supports the above statement; the complex impedance plots at different temperatures explain the increase of M' and M''. The electrode surface polarization phenomena (i.e., tilted spike) is often separated from the bulk material (i.e., depressed semicircle) in the complex impedance plots (Z'' *vs.* Z').[30]

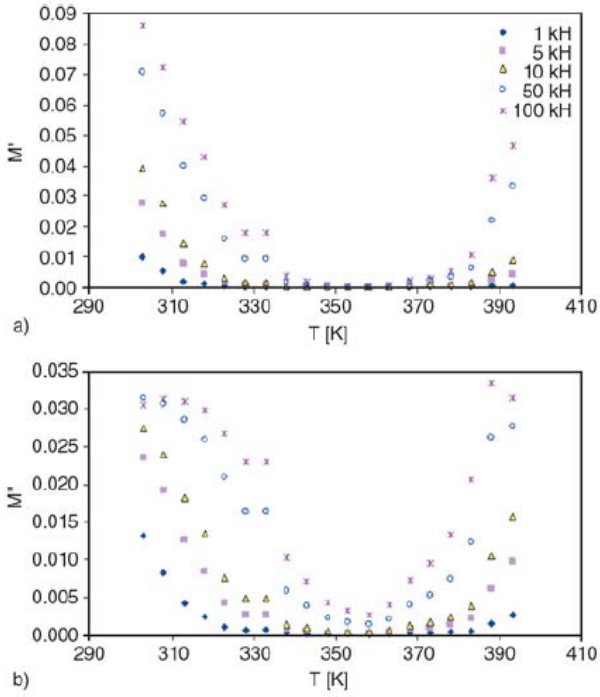

Figure 7. Temperature dependence of (a) M' and (b) M'' at selected frequencies for chitosan-silver triflate (90:10) composite

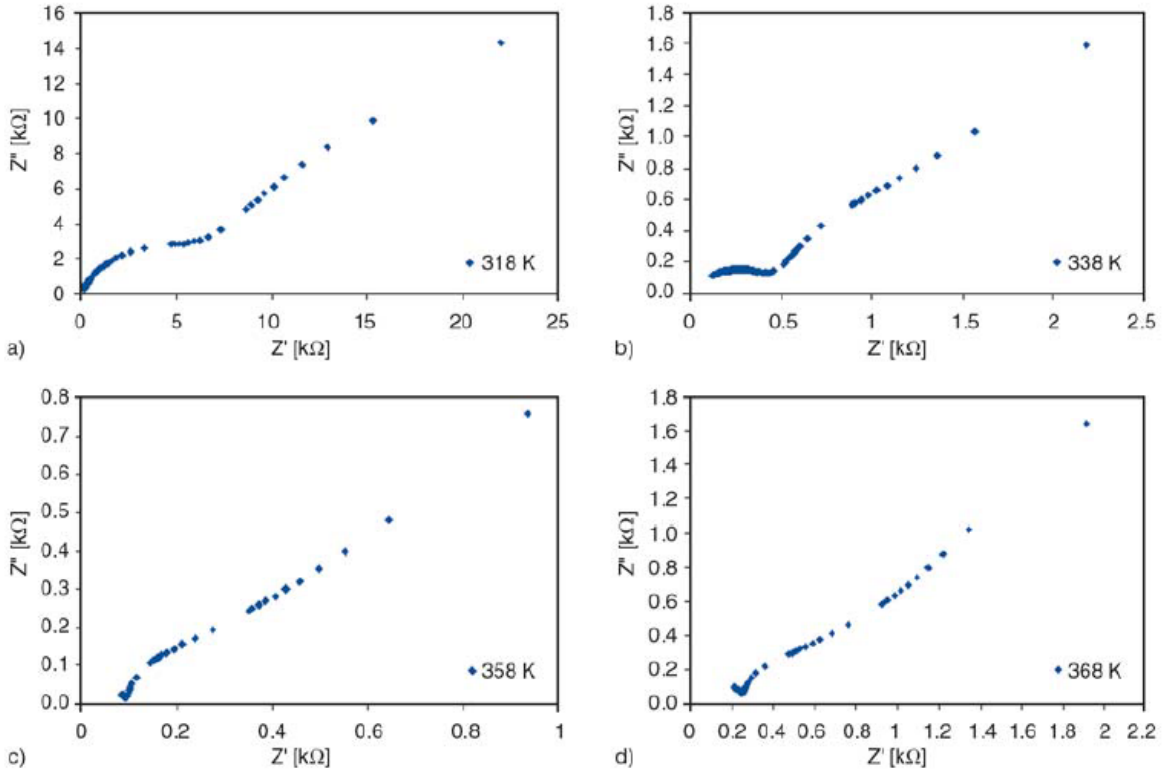

Figure 8. Complex impedance of chitosan-silver triflate (90:10) composite at selected temperatures

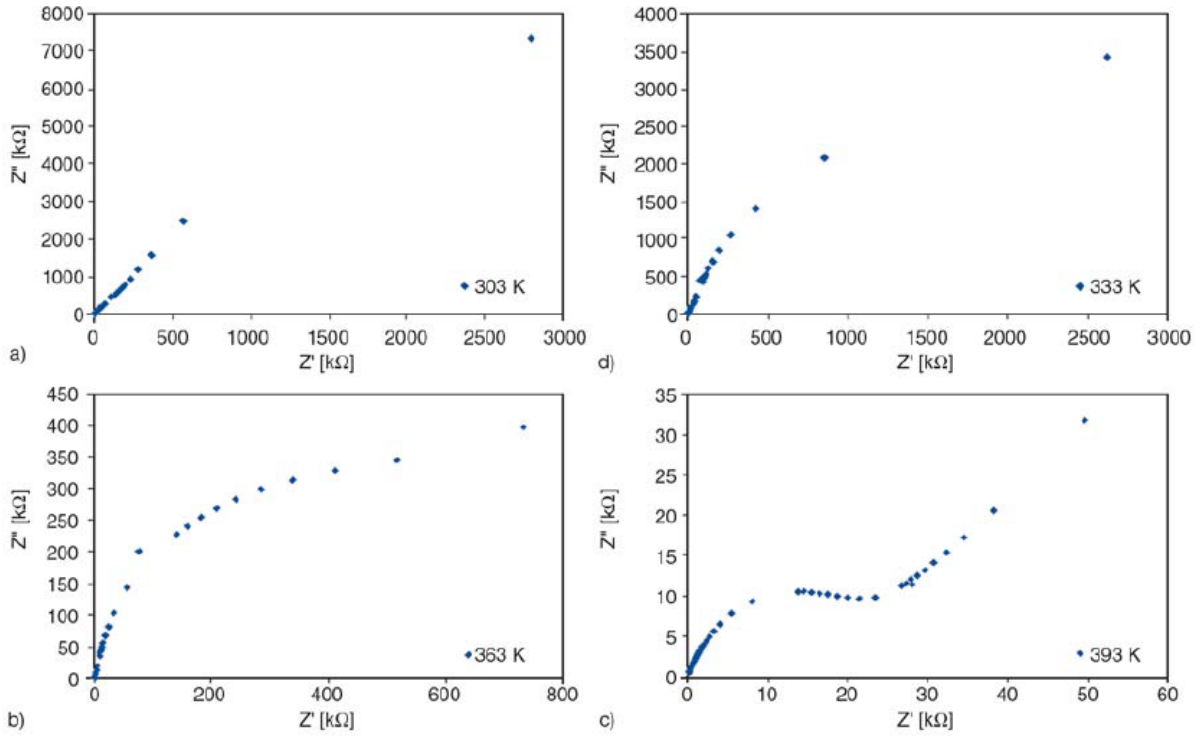

Figure 9. Complex impedance plots of pure chitosan at selected temperatures

The free charges are building up in the interface of the electrode surfaces and the electrolyte form an electric double layer (EDL) capacitance that results in the formation of electrode polarization phenomena (tilted spike).[30,22] The silver nanoparticles act as grain boundaries causing second semicircles to appear at different temperatures (Figure 8). It can be concluded that the silver nanoparticles and silver ions compete. As the temperature rises from 303 to 358 K, the bulk resistance decreases, i.e., silver ions are dominant and the system behaves as an ionic conductor. However, when the temperature passes 358 K, the bulk resistance increases since more silver nanoparticles are formed from silver ions. Subsequently, both M' and M'' increase since the conduction mechanism and overall polarization decrease because of the decline in silver ion amounts. Z' and Z'' increase above 358 K. At this point, a noncomposite behavior seems to be appeared due the polymer electrolyte rather than ionic behavior. On the other hand, in pure chitosan (Figure 9), the second semicircles cannot be seen.

The complex impedance plot of pure chitosan is shown in Figure 9 at different temperatures. The bulk resistance of chitosan-silver triflate (90:10) solid electrolyte is lower than that of pure chitosan. Also, there is a continuous decrease in pure chitosan's bulk resistance as the temperature increases up to 393 K. It is a difference comparing that to the Z''–Z' plot of chitosan-silver triflate (90:10) solid electrolyte. Another observation would be that pure chitosan in its Z''–Z' plot does not manifest second semicircles as temperature changes.

Specific UV-vis absorption band can be seen for silver nanoparticles and their clusters in the ultraviolet-visible region.[31] The UV-Vis absorption spectra at temperature 303 K for chitosan-silver triflate (90:10) solid electrolyte and pure chitosan are shown in Figure 10.

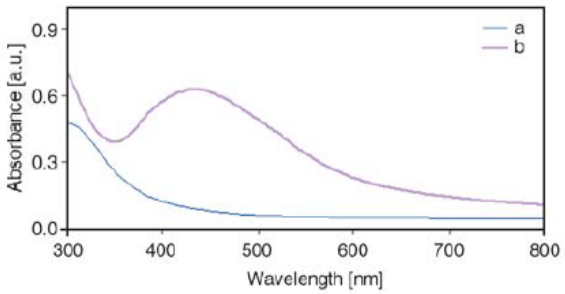

Figure 10. UV-Vis absorption spectra of (a) pure chitosan and (b) chitosan- CF_3SO_3Ag (90:10) composite at 303 K.

The chitosan-silver triflate (90:10) solid electrolyte has a broad absorption peak from 400 to 500 nm with maximum being at 426 nm, mainly due to the surface plasmon band of silver nanoparticles. Pure chitosan has no specific absorption peak within this wavelength range. The concentration of the silver nanoparticles corresponds with the height of the peak.[32,33]

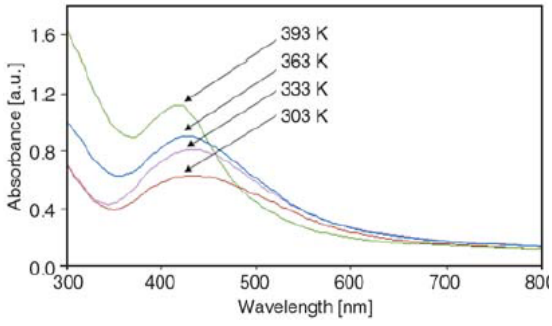

Figure 11. UV-Vis absorption spectra of chitosan- CF_3SO_3Ag (90:10) composite at different temperatures

The UV-Vis absorption spectra of chitosan-silver triflate (90:10) solid electrolyte at different temperatures is shown in Figure 11. As the temperature increases from 303 K to 393 K, the peak heights increase from 0.61 to 1.2. It shows that at high temperatures, more rapid conversion of silver ions to silver nanoparticles occurs.[34] It has been reported that the silver ion reduction can occur in hydroxyl, carboxyl and imide group-containing polymers.[35,36] The color change of solid membranes from yellow to dark brown is another indicator of silver nanoparticle formation. Similar behavior for PVP-silver salt electrolyte was mentioned by Kang *et al*.[37] Interacting electromagnetic field causes the free conduction electrons to oscillate (surface plasmon resonance (SPR)).[38] The intense color in the visible spectrum can only be seen in electrodes with plasmon resonance since they have free electrons.[39]

The presence of silver nanoparticle was confirmed with transmission electron microscopy (TEM). The silver nanoparticles within chitosan- CF_3SO_3Ag (90:10) solid electrolyte can be seen in Figure 12. It can be seen that they are agglomerated and dispersed. When the repulsion energy is lower than the attraction energy between the particles, it leads to particle agglomeration.[40]

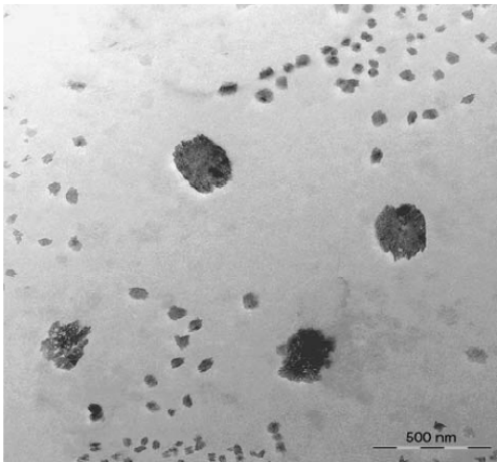

Figure 12. TEM micrograph of silver nanoparticles for chitosan-silver triflate (90:10) composite at room temperature

As far as we know, change in properties of solid polymer electrolytes (SPE) by the effect of silver ion reduction to silver nanoparticles is reported for the first time.

Scaling behavior of M".

More information can be obtained on the effect of charge carrier concentration, structure, and temperature on relaxation dynamics by studying the scaling of electric modulus.[41] Figure 13 shows the electric modulus of chitosan-silver triflate (90:10) as its imaginary part is scaled at different temperatures. The parameters of M'' and f are scaled according to M''_{max} and f_{max}, respectively.

A single master curve is formed by merging of all the modulus spectra (Figure 13). For the particular compositions, the dynamical relaxation is independent on temperature.[42] Deviation from Debye behavior can be seen from the dielectric relaxation processes evidenced by the asymmetric plot shape and the non-symmetric distribution of relaxation times.[43] A clear non-symmetric plot can be seen for the normalized modulus in Figure 13, in accordance with the non-exponential behavior of electrical functions.[44]

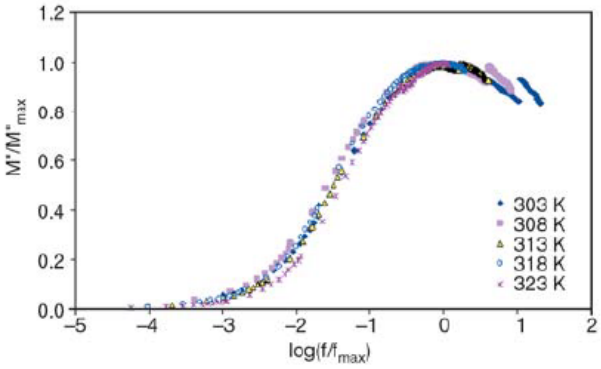

Figure 13. Scaling of M″ for chitosan-silver triflate (90:10) composite at different temperatures

The deviation from Debye relaxation can be shown from the exponent β. The typical Debye behavior is 1.14 decades, while in the chitosan:CF_3SO_3Ag (90:10) composite full-width half height (FWHH) is nearly 2 decades. A highly non-exponential conductivity relaxation is concluded from the small value (0.57) of β.[42] Deviation from Debye-type relaxation becomes the more significant the lower the value of β (standard value is β=1). A practical solid electrolyte has a β value of less than 1.[20]

Conclusions

A solution casting preparation of chitosan-silver triflate electrolytes resulted in composite films. The highest conductivity samples have no shift towards higher frequency in their M'' spectra due to a low number of mobile charge carriers. The systems capacitive nature is demonstrated by the long tail of M' spectra in the low-frequency range. Non-Debye relaxation type can be seen from the broad peaks of M″ spectra. Relaxation times distribution gives a deformed arc shape of Argand plots. A large amount of silver nanoparticles formed from silver ions at higher temperatures causing the increase of M' and M'' values. The presence and growth of silver nanoparticles result in the appearance of the temperature dependence of second semicircles in complex impedance plots. UV-Vis and transmission electron microscopy (TEM) confirmed the formation of silver nanoparticles. A temperature independent nature of the dynamical relaxation processes was demonstrated and a highly non-exponential nature of the conductivity relaxation is concluded from the value of the β exponent.

References

[1]Karan, N. K., Pradhan, D. K., Thomas, R., Natesan, B., Katiyar, R. S., Solid polymer electrolytes based on polyethylene oxide and lithium trifluoro- methanesulfonate (PEO-$LiCF_3SO_3$): Ionic conductivity and dielectric relaxation. *Solid State Ionics*, **2008**, *179*, 689–696. DOI: 10.1016/j.ssi.2008.04.034

[2]Dieterich, W., Dürr, O., Pendzig, P., Bunde, A., Nitzan, A., Percolation concepts in solid state ionics. *Physica A:*

Statistical Theoret. Phys., **1999**, *266*, 229–237. DOI: 10.1016/S0378-4371(98)00597-4

[3]Yahya, M. Z. A., Arof, A. K., Studies on lithium acetate doped chitosan conducting polymer system. *Eur. Polym. J.*, **2002**, *38*, 1191–1197. DOI: 10.1016/S0014-3057(01)00290-7

[4]Bhargav, P. B., Mohan, V. M., Sharma, A. K., Rao, V. V. R. N., Investigations on electrical properties of (PVA:NaF) polymer electrolytes for electrochemical cell applications. *Curr. Appl. Phys.*, **2009**, *9*, 165–171. DOI: 10.1016/j.cap.2008.01.006

[5]Baskaran, R., Selvasekarapandian, S., Kuata, N., Kawamura, J., Hattori, T., Ac impedance, DSC and FT-IR investigations on (x)PVAc-(1–x)PVdF blends with $LiClO_4$. *Mater. Chem. Phys.*, **2006**, *98*, 55–61. DOI: 10.1016/j.matchemphys.2005.08.063

[6]de Jonge J. J., Van Zon A., de Leeuw S. W., Molecular dynamics study of the influence of the polarizability in PEOx-NaI polymer electrolyte systems. *Solid State Ionics*, **2002**, *147*, 349–359. DOI: 10.1016/S0167-2738(02)00056-5

[7]Avellaned, C. O. A., Vieira, D. F., Al-Kahlout, A., Leite, E. R., Pawlicka, A., Aegerter, M. A., Solid-state electrochromic devices with Nb_2O_5:Mo thin film and gelatin-based electrolyte. *Electrochim. Acta*, **2007**, *53*, 1648– 1654. DOI: 0.1016/j.electacta.2007.05.065

[8]Natesan, B., Karan, N. K., Katiyar, R. S.: Ion relaxation dynamics and nearly constant loss behavior in polymer electrolyte. *Phys. Review E*, **2006**, *48*, 042801/1– 042801/4. DOI: 10.1103/PhysRevE.74.042801

[9]Singh, K. P., Gupta, P. N., Study of dielectric relaxation in polymer electrolytes. *Eur. Polym. J.*, **1998**, *34*, 1023–1029. DOI: 10.1016/S0014-3057(97)00207-3

[10]Chabchoub, N., Khemakhem, H., Ac ionic conductivity investigations on the $CsK(SO_4)$-$Te(OH)_6$ material. J. Alloys Compd., **2004**, *370*, 8–17. DOI: 10.1016/j.jallcom.2003.08.091

[11]Richert, R., The modulus of dielectric and conductive materials and its modification by high electric fields. J. Non-Cryst. Solids, **2002**, *305*, 29–39. DOI: 10.1016/S0022-3093(02)01085-2

[12]Molak, A., Paluch, M., Pawlus, S., Klimontko, J., Ujma, Z., Gruszka, I.: Electric modulus approach to the analysis of electric relaxation in highly conducting $(Na_{0.75}Bi_{0.25})(Mn_{0.25}Nb_{0.75})O_3$ ceramics. *J. Appl. Phys. D: Appl. Phys.*, **2005**, *38*, 1450–146. DOI: 10.1088/0022-3727/38/9/019

[13]Migahed, M. D., Ishra, M., Fahmy, T., Barakat, A., Electric modulus and AC conductivity studies in conducting PPy composite films at low temperature. *J. Phys. Chem. Solids*, **2004**, *65*, 1121–1125. DOI: 10.1016/j.jpcs.2003.11.039

[14]Majid, S. R., Arof, A. K., Electrical behavior of proton-conducting chitosan-phosphoric acid-based electrolytes. *Physica B: Condensed Matter*, **2007**, *390*, 209–215. DOI: 10.1016/j.physb.2006.08.038

[15]Kim, J. H., Min, B. R., Wong, J., Kang, Y. S., Anomalous temperature dependence of facilitated propylene transport in silver polymer electrolyte membranes. *J. Membrane Sci.*, **2003**, *227*, 197–206. DOI: 10.1016/j.memsci.2003.08.026

[16]Kang, S. W., Kim, J. H., Won, J., Char, K., Kang, Y. S., Effect of amino acids in polymer/silver salt complex membranes on facilitated olefin transport. *J. Membrane Sci.*, **2004**, *248*, 201–206 (2004). DOI: 10.1016/j.memsci.2004.08.028

[17]Kim, J. H., Wong, J., Kang, Y. S., Olefin-induced dissolution of silver salts physically dispersed in inert polymers and their application to olefin/paraffin separation. *J. Membrane Sci.*, **2004**, *241*, 403–407. DOI: 10.1016/j.memsci.2004.05.027

[18]Lim, P. Y., Liu, R. S., She, P. L., Hung, C. F., Shih, H. C., Synthesis of Ag nanospheres particles in ethylene glycol by electrochemical-assisted polyol process, *Chem. Phys. Lett.*, **2006**, *420*, 304–308. DOI: 10.1016/j.cplett.2005.12.075

[19]Padmasree, K. P., Kanchan, D. K., Modulus studies ofCdI_2–Ag_2O–V_2O_5–B_2O_3 system. *Mater. Sci. Eng. B*, **2005**, *122*, 24–28 (2005). DOI: 10.1016/j.mseb.2005.04.011

[20]Ram, M., Chakrabarti, S., Dielectric and modulus studies on $LiFe_{1/2}Co_{1/2}VO_4$. *J. Alloys Compd.*, **2008**, *462*, 214–219. DOI: 10.1016/j.jallcom.2007.08.001

[21]Yahya M. Z. A., Arof, A. K., Conductivity and X-ray photoelectron studies on lithium acetate doped chitosan films. *Carbohydrate Polym.*, **2004**, *55*, 95–100. DOI: 10.1016/j.carbpol.2003.08.018

[22]Pradhan, D. K., Choudhary, R. N. P., Samantaray, B. K., Studies of the structural, thermal and electrical behavior of polymer nanocomposite electrolytes. *Express Polym. Lett.*, **2008**, *2*, 630–638. DOI: 10.3144/expresspolymlett.2008.76

[23]Yakuphanoglu, F., Electrical conductivity and electrical modulus properties of dihexylsexithiophene organic semiconductor. *Physica B*, **2007**, *393*, 139–142. DOI: 10.1016/j.physb.2006.12.075

[24]Dutta, A., Sinha, T. P., Jena, P., Adak, S., Ac conductivity and dielectric relaxation in ionically conducting soda-lime-silicate glasses. *J. Non-Cryst. Solids*, **2008**, *354*, 3952–3957. DOI: 10.1016/j.jnoncrysol.2008.05.028

[25]Patro, L. N., Hariharan, K., AC conductivity and scaling studies of polycrystalline SnF_2. *Mater. Chem. Phys.*, **2009**, *116*, 81–87. DOI: 10.1016/j.matchemphys.2009.0

[26]Patro, L. N., Hariharan, K.: Frequency-dependent conduction characteristics of mechanochemically synthesized $NaSn_2F_5$. *Mater. Sci. Eng., B*, **2009**, *162*, 173–178. DOI: 10.1016/j.mseb.2009.04.003

[27]Kwan, K. C., *Dielectric phenomena in solids*. Elsevier, New York, 2004.

[28]Calleja, R. D., Matveeva, E. S., Parkhutik, V. P., Electric relaxation in chemically synthesized polyaniline: Study using electric modulus formalism. *J. Non-Cryst. Solids*, **1995**, *180*, 260–265. DOI: 10.1016/0022-3093(94)00470-6

[29]Psarras, G. C., Gatos, K. G., Karahaliou, P. K., Georga, S. N., Krontiras, C. A., Karger-Kocsis, J., Relaxation phenomena in rubber/layered silicate nanocomposites. *Express Polym. Lett.*, **2007**, *1*, 837–845. DOI: 10.3144/expresspolymlett.2007.116

[30]Sengwa, R. J., Choudhary, S., Sankhla, S.: Low-frequency dielectric relaxation processes and ionic conductivity of montmorillonite clay nanoparticles colloidal suspension in poly(vinyl pyrrolidone)-ethylene glycol blends. *Express Polym. Lett.*, **2008**, *2*, 800–809. DOI: 10.3144/expresspolymlett.2008.93

[31]Lu, J., Suarez, J. J. B., Takahashi, A., Haruta, M., Oyama, S. T., In situ UV-vis studies of the effect of particle size on the epoxidation of ethylene and propylene on supported silver catalysts with molecular oxygen. *J. Catal.*, **2005**, *232*, 285–295 (2005). DOI: 10.1016/j.jcat.2005.02.013

[32]Kim, J. H., Kim, C. K., Won, J., Kang, Y. S., Role of anions for the reduction behavior of silver ions in polymer/silver salt complex membranes. *J. Membrane Sci.*, **2005**, *250*, 207–214 (2005). DOI: 10.1016/j.memsci.2004.10.032

[33]Liu, Y., Chen, S., Zhong, L., Wu, G., Preparation of high-stable silver nanoparticle dispersion by using sodium alginate as a stabilizer under gamma radiation. *Radiat. Phys. Chem.*, **2009**, *78*, 251–255. DOI: 10.1016/j.radphyschem.2009.01.003

[34]Kim, J. H., Min, B. R., Kim, H. S., Won, J., Kang, Y. S., Facilitated transport of ethylene across polymer membranes containing silver salt: Effect of HBF_4 on the photoreduction of silver ions. *J. Membrane Sci.*, **2003**, *212*, 283–288. DOI: 10.1016/S0376-7388(02)00451-9

[35]Sharma, V. K., Yngard, R. A., Lin, Y., Silver nanoparticles: Green synthesis and their antimicrobial activities. *Adv. Colloid Interface Sci.*, **2009**, *145*, 83–96. DOI: 10.1016/j.cis.2008.09.002

[36]Silvert, P-Y., Herrera-Urbina, R., Duvauchelle, N., Vijayakrishnan, V., Elhsissen, K. T., Preparation of colloidal silver dispersions by the polyol process. Part 1 – Synthesis and characterization. *J. Mater. Chem.*, **1997**, *7*, 293–299 (1997). DOI: 10.1039/JM9960600573

[37]Kang, S. W., Kim, J. H., Oh, K., Won, S. J., Char, K., Kim, H. S., Kang, Y. S. Highly stabilized silver polymer electrolytes and their application to facilitated olefin transport membranes. *J. Membrane Sci.*, **2004**, *236*, 163–169. DOI: 10.1016/j.memsci.2004.02.020

[38]Srivastava, S., Haridas, M., Basu, J. K., Optical properties of polymer nanocomposites. *Bull. Mater. Sci.*, **2008**, **31**, 213–217. DOI https://doi.org/10.1007/s12034-008-0038-9

[39]Zieli´nska, A., Skwarek, E., Zaleska, A., Gazda, M., Hupka, J., Preparation of silver nanoparticles with controlled particle size. *Procedia Chem.*, **2009**, *1*, 1560–1566. DOI: 10.1016/j.proche.2009.11.004

[40]Lin, H-W., Hwu, W-H., Ger, M-D., The dispersion of silver nanoparticles with physical dispersal procedures. *J. Mater. Process. Technol.*, **2008**, *206*, 56–61. DOI: 10.1016/j.jmatprotec.2007.12.025

Received: 19.05.2019
Accepted: 15.07.2019